Journal of Inorganic Biochemistry 175 (2017) 179–189

Contents lists available at ScienceDirect

Journal of Inorganic Biochemistry

journal homepage: www.elsevier.com/locate/jinorgbio

The potent anti-cancer activity of *Dioclea lasiocarpa* lectin

Ana C.S. Gondim[a,b,c,1], Isolda Romero-Canelón[b], Eduardo H.S. Sousa[b,c], Claudia A. Blindauer[b], Jennifer S. Butler[b], María J. Romero[b,2], Carlos Sanchez-Cano[b], Bruno L. Sousa[a], Renata P. Chaves[d], Celso S. Nagano[d], Benildo S. Cavada[a,*], Peter J. Sadler[b,*]

[a] Department of Biochemistry and Molecular Biology, Federal University of Ceará, 60455-760 Fortaleza, Ceará, Brazil
[b] Department of Chemistry, University of Warwick, Coventry CV4 7AL, UK
[c] Department of Organic and Inorganic Chemistry, Federal University of Ceará, 60455-900 Fortaleza, Ceará, Brazil
[d] Department of Fishing and Engineering, Federal University of Ceará, 60455-900 Fortaleza, Ceará, Brazil

ARTICLE INFO

Keywords:
Metalloprotein
Legume lectin
Homology model
Anticancer
Apoptosis

ABSTRACT

The lectin DLasiL was isolated from seeds of the *Dioclea lasiocarpa* collected from the northeast coast of Brazil and characterized for the first time by mass spectrometry, DNA sequencing, inductively coupled plasma-mass spectrometry, electron paramagnetic resonance, and fluorescence spectroscopy. The structure of DLasiL lectin obtained by homology modelling suggested strong conservation of the dinuclear Ca/Mn and sugar-binding sites, and dependence of the solvent accessibility of tryptophan-88 on the oligomerisation state of the protein. DLasiL showed highly potent (low nanomolar) antiproliferative activity against several human carcinoma cell lines including A2780 (ovarian), A549 (lung), MCF-7 (breast) and PC3 (prostate), and was as, or more, potent than the lectins ConBr (*Canavalia brasiliensis*), ConM (*Canavalia maritima*) and DSclerL (*Dioclea sclerocarpa*) against A2780 and PC3 cells. Interestingly, DLasiL lectin caused a G2/M arrest in A2780 cells after 24 h exposure, activating caspase 9 and delaying the on-set of apoptosis. Confocal microscopy showed that fluorescently-labelled DLasiL localized around the nuclei of A2780 cells at lectin doses of 0.5–2 × IC_{50} and gave rise to enlarged nuclei and spreading of the cells at high doses. These data reveal the interesting antiproliferative activity of DLasiL lectin, and suggest that further investigations to explore the potential of DLasiL as a new anticancer agent are warranted.

1. Introduction

Cancer is the leading cause of morbidity and mortality around the world, with approximately 14 million new cases and 8.2 million cancer related deaths worldwide in 2012 [1]. Furthermore, the number of new cases in developed countries is expected to rise up to 70% in the next decades [1], due to population ageing and growth [2]. Hence there is a need for discovery of new anticancer drugs, especially those with novel mechanisms of action that can combat resistance.

There is increasing interest in the role of glycans on the surface of tumour cells in relation to tumour cell division, migration (metastasis) and recognition by the immune system (lymphocytes) [3]. Cancer cells show many altered glycosylation patterns including those of cell surface biomolecules, such as glycolipids and glycoproteins, which may affect a range of processes including the transcription of genes, trafficking, or retention of biomolecules [4]. These aberrant changes provide a basis for the discovery of biomarkers and therapeutic agents capable of targeting cells by recognizing particular glycosylation patterns.

Lectins are carbohydrate-binding proteins that fulfil multiple biological roles. They are ubiquitously distributed in nature, being found in vertebrates, invertebrates, bacteria, viruses and plants. These proteins bind specifically to certain sugars, glycoproteins and glycolipids, and have a variety of functions in mammals, for example roles on cell surfaces and in the immune system. In general, plant lectins have been used in cell biology and immunology as diagnostics [5] and as immunomodulatory agents [6], as well as for therapeutic purposes [4]. Lectins have potential as oral drugs since they are often resistant to digestion. Importantly they survive passage through the gut, bind to gastrointestinal cells, enter the circulation intact, and maintain their biological activity [7]. Plant lectins from nuts and seeds are the most widely studied, especially Concanavalin A (ConA), a homo-tetramer (4 × 26.5 kDa) with Mn(II) and Ca(II) ions bound at 4 binuclear

* Corresponding authors.
E-mail addresses: bscavada@gmail.com (B.S. Cavada), p.j.sadler@warwick.ac.uk (P.J. Sadler).
[1] Current address: Department of Organic and Inorganic Chemistry, Federal University of Ceará, 60455-900, Fortaleza, Ceará, Brazil.
[2] Current address: Departamento de Química Inorgánica, Facultade de Química, Universidade de Santiago de Compostela, 15782, Santiago de Compostela, Spain.

http://dx.doi.org/10.1016/j.jinorgbio.2017.07.011
Received 29 March 2017; Received in revised form 3 July 2017; Accepted 10 July 2017
Available online 16 July 2017

binding sites per tetramer, and with specificity for mannosyl and glycosyl sugars [8,9]. Interestingly, despite the high similarity amongst plant lectins, many have shown remarkably distinct biological profiles, with a vast range of biological activities which include anti-inflammatory [10], antidepressive [11], anticonceptive [12] and vasodilatory activities [8]. A few lectins have been recently identified as promising antitumour agents, for example ConA and the lectin ML-I from mistletoe are in pre-clinical and clinical trials for human liver cancer and malignant melanoma [13,14].

Lectins appear to inhibit tumour growth in vitro and in vivo by preferential binding to cell membranes of cancer cells or to their receptors [7,15,16]. Nevertheless, this binding leads to different cellular effects that depend on the lectin, such as the activation of protein kinases, or alteration of the production of interleukins leading to immunological responses [7]. Additionally, plant lectins also have a role in triggering different cell death pathways, including apoptosis, necrosis and/or autophagy [3,7,14,17–19]. For example, ML-I (Mistletoe lectin I from *Viscum album*) and Ricin A (from *Ricinus communis*) bind to ribosomes and inhibit protein synthesis in vitro, while RBA (Rice bran agglutinin) or WGA (Wheat germ agglutinin) induce G2/M cell cycle arrest and downstream apoptosis [7]. BFL (from *Bauhinia forficata*) has potent anticancer activity towards MCF-7 cancer cells, causing DNA fragmentation and cell cycle arrest at the G2/M phase, along with inhibition of caspase 9 leading to primary and secondary necrosis [20]. However, determination of their mechanism of action is not always straightforward. Another similar lectin BG2 (from *Bauhinia variegata*) inhibits cell proliferation of MCF-7 breast cancer cells and HepG2 hepatomas, displaying IC_{50} values of 0.18 and 1.4 μM, respectively, but its cellular behaviour and mechanism of action have not yet been elucidated [21].

Recently, we isolated DLasiL from the seed pods of *Dioclea lasiocarpa*, a flowering plant found in Northeastern Brazil. DLasiL is a ConA-like seed lectin with high binding specificity for glucose/mannose and shows contractile activity on isolated rat aorta with possible involvement of endothelium-derived factors [22]. However, this lectin has not been thoroughly characterized, nor its detailed biological properties explored. Here we investigate the potential of DLasiL as an anticancer agent by studying its antiproliferative activity, cell cycle effects and cell death processes in A2780 ovarian, A549 lung, PC3 prostate and MCF-7 breast human cancer cell lines.

2. Material and methods

2.1. Lectin purification

The lectins were extracted from seeds of *Canavalia brasiliensis*, *Canavalia maritima*, *Dioclea lasiocarpa* and *Dioclea sclerocarpa*. The protein extractions were performed on fine seed powders, prepared for each species, at ambient temperature by stirring for 4 h in 0.1 M Tris-HCl buffer pH 7.4 with 0.15 M NaCl. The crude extract was then filtered and centrifuged at 10,000 × *g* for 30 min. The pellet was discarded and the supernatant was transferred to a Sephadex G-50 column previously equilibrated with 0.1 M Tris-HCl buffer pH 7.4 with 0.15 M NaCl, 5 mM $CaCl_2$, and 5 mM $MnCl_2$. The retained fraction corresponding to the purified protein was eluted with 0.2 M glucose containing 0.15 M NaCl, and subsequently dialyzed against water, lyophilized, and stored at ambient temperature. Protein concentration and purity were analyzed by the Bradford method, electronic absorption spectroscopy and SDS-PAGE [23,24].

2.2. Protein digestion and tandem mass spectrometry analysis

After a 12% SDS-PAGE, DLasiL bands were excised and bleached in a solution of 50 mM ammonium bicarbonate in 50% *v*/v acetonitrile. The bands were then dehydrated in 100% acetonitrile and dried in a Speedvac (LabConco). The gel was rehydrated overnight at 310 K with a solution of 50 mM ammonium bicarbonate, pH 8.0, containing trypsin (Promega; 1:50 w/w enzyme:substrate ratio). The peptides were extracted from the gel and concentrated, followed by injection into a NanoAcquity system (Waters, Corp., Milford, USA) connected to the electrospray source of a mass spectrometer (SYNAPT HDMS system; Waters Corp., Milford, CT, USA). The sample was applied to a C18 chromatography column (75 μm × 100 mm) and eluted with a 10–85% acetonitrile gradient containing 0.1% formic acid. The mass spectrometer was operated in positive mode with 363 K source temperature and 3.0 kV capillary voltage. The LC-MS/MS experiment was performed with the DDA (data dependent analysis) function, which selects doubly- or triply-charged precursor ions, for fragmentation by collision-induced dissociation (CID). The data were processed and analyzed with ProteinLynx v2.4 (Waters) using the peptide fragmentation pattern as search parameter. Some peptide sequences were determined by manual de novo sequencing. Primary structure alignments were made with ESPript 2.2 [25].

2.3. DLasiL gene cloning and sequencing

Genomic DNA was isolated from young leaves of *Dioclea lasiocarpa* using a method based on the detergent cetyltrimethylammonium bromide (CTAB). The DLasiL gene was amplified by PCR using specific primers, D_forward (TCA AA AAA ATC TCT GAT G) and D_reverse (TCA GAC GAC GGA TGC AAT), designed based on the N- and C-terminal sequences of Diocleinae lectins. The amplified fragment was purified using the kitPureLink™ QuickGel Extration (Invitrogen™/Life Technologies) and cloned into pGEM-T *Easy Vector* (Promega, USA). *Escherichia coli* DH5α cells (Novagen) were transformed by electroporation with an Eppendorf 2510 electroporator, following the manufacturer's instructions. The construct DlasiL:pGEM-T was sequenced with an MegaBASE 1000 DNA sequencer (GE-Healthcare). The reads were analyzed by the Phred-Phrap-Consed package.

2.4. Electron paramagnetic resonance spectroscopy

Electron paramagnetic resonance spectroscopy (EPR) was used to confirm the presence of Mn(II) in the leguminous lectins ConBr, ConM, DLasiL and DSclerL. Solutions containing ca. 0.4 mM of proteins were made up from the lyophilized powders in Milli-Q water; no buffer was used.

All EPR spectra were recorded on aqueous samples (150 μL) on a Bruker EMX (X-band) spectrometer at ambient temperature (ca. 291 K) in a cylindrical Tm110 mode cavity (Bruker 4103TM). Spectrosil quartz tubes with inner diameter of 1.0 and 1.2 mm were used, sealed with T-Blu Tac®, and placed inside a larger quartz tube (O.D. 2.0 mm). The EPR parameters were: modulation amplitude 10 G, microwave power 0.63 mW, 6.3×10^5 receiver gain, sweep gain 40.96 s with resolution 2048 resolution in X. The spectra were analyzed by the software Bruker WINEPR.

2.5. Inductively coupled plasma-mass spectrometry

The metal content of purified ConBr, ConM, DLasiL and DSclerL lectins was determined by inductively coupled plasma-mass spectrometry (ICP-MS) using an Agilent 7500cx instrument with an IAS (integrated auto sampler). The parameters were: plasma gas flow (argon): 15 L/min, auxiliary gas: 0.9 L/min, forward power 1550 W, ORC (octopole reaction cell) used in helium mode (Tune file 1), no ORC (Tune file 2), internal standard ^{166}Er; no other corrections were used and sample delivery was 0.3 rps. The lectins were digested by treatment with 5% v/v of nitric acid for 1 h and diluted with double deionized water (DDW). The metal isotopes detected were ^{12}Mg, ^{20}Ca, ^{25}Mn, ^{27}Co, ^{28}Ni, ^{30}Zn. Only ^{12}Mg, ^{20}Ca, ^{25}Mn were found in significant amounts for precise quantitation. Standards used in the experiments were purchased from Sigma Aldrich and freshly prepared for each experiment.

2.6. Fluorescence spectroscopy

Steady-state fluorescence emission measurements were obtained on a Jasco FP 6500 (Jasco International Co., Ltd., Tokyo, Japan), equipped with a 150 W xenon lamp, using a quartz cuvette (volume 500 μL; pathlength 1 cm). The slit widths on the excitation and emission monochromators were 5 and 10 nm, respectively. To excite tryptophan residues of the proteins, the samples were irradiated at 295 nm with $OD_{295nm} \leq 0.05$; the emission spectra were recorded between 305 and 450 nm. Titrations of DLasiL solutions with aliquots of quenchers or fluorophore stocks, such as acrylamide, cesium chloride, and potassium iodide were carried out. Briefly, the decrease of fluorescence intensity was observed after serial addition of small aliquots of freshly prepared stocks of quenchers to a buffered solution of DLasiL (in 10 mM phosphate-buffered saline solution containing 2.7 mM NaCl) in a cuvette, followed by mixing and incubation for 2 min in the sample compartment in the dark. Sodium thiosulfate (0.2 mM final concentration), was added to the iodide stock solution to avoid formation of triiodide (I_3^-) as described elsewhere [26]. Experiments with denatured DLasiL were performed by pre-treating the protein with 6 M Gdn·HCl at room temperature for 12 h. All the spectra were corrected, subtracted with appropriate blank without DLasiL and experiments were performed in duplicate at 298 K. Quenching data were analyzed by fitting to the Stern–Volmer equation [27]:

$$F_0/F = 1 + K_{SV}[Q],$$

where F_0 and F are the fluorescence intensities at the maximum of the protein emission bands in the absence and presence of the quencher, respectively, [Q] is the molar quencher concentration and K_{SV} is the Stern–Volmer quenching constant. The modified Stern-Volmer equation was also tested, but did not improve the fit.

2.7. Circular dichroism spectroscopy

Circular dichroism (CD) spectra were obtained on a Jasco J-810 spectropolarimeter (Jasco International Co., Ltd., Tokyo, Japan) equipped with a Peltier thermostat, using a 1 mm pathlength rectangular quartz cell. A DLasiL concentration of ca. 10 μM was used for recording CD spectra in the near-UV region (300–250 nm). The thermal unfolding properties of DLasiL were investigated by recording CD spectra in the near-UV region at various temperatures. All experiments were performed in 10 mM sodium phosphate buffer at pH 7.4 in the absence or presence of mannose or glucose to investigate binding and structural changes.

2.8. Homology modelling

The most suitable template for *Dioclea lasiocarpa* lectin was identified using the remote homology recognition server Phyre [28], which also produces multiple and pairwise sequence alignments. The template structure with the highest % identity (96%) was pdb 1H9W, for a seed lectin from *Dioclea guianensis* [29]. Due to the extremely high similarity between model and template sequence, the homology model generated by the Phyre server was used for inspecting tryptophan, metal, and saccharide environments without further manipulations. The physical soundness of the model was checked using the WHATIF web interface (http://swift.cmbi.ru.nl/servers/html/index.html). To explore tryptophan environments in the functional biological assembly, pdb 4H55 (containing a monomer in the asymmetric unit) was analyzed using the pdbePISA server at EBI (http://www.ebi.ac.uk/pdbe/pisa/). This yielded the desired tetrameric assembly [30] shown in Fig. S6. In addition, the dimeric structure from pdb 1H9W was also inspected in this regard.

Structural overlays and comparisons were performed in Swiss pdb viewer v. 3.7, and structural images were generated either in the latter program or in MOLMOL v. 2k.1 [31].

2.9. Cell culture

Human ovarian carcinoma (A2780), human Caucasian lung carcinoma (A549), human prostate carcinoma (PC3) and human breast carcinoma (MCF-7) were purchased from ECACC (European Collection of Animal Cell Culture, Salisbury, UK). A2780 and PC3 cells were cultured in Roswell Park Memorial Institute medium (RPMI-1640) while A549 and MCF-7 were kept in Dulbecco's Modified Eagle medium (DMEM). Both cell-culture media were supplemented with 10% v/v of foetal calf serum, 1% v/v of L-glutamine and 1% v/v penicillin/streptomycin, and cells were grown as single monolayers at 310 K in a humidified atmosphere containing 5% CO_2. The cells were sub-cultured at regular intervals, the passages were made by trypsinizing the cells when 80–90% of confluence was achieved. For all assays involving lectins, medium with only 1% foetal calf serum was used to avoid lectin deactivation by non-specific protein binding.

2.10. Cell viability assays

The antiproliferative activity of the lectins (ConBr, ConM, DLasiL and DSclerL) towards A2780, A549, PC3 and MCF-7 cancer cell lines was determined by measuring IC_{50} values using the SRB assay to determine cell viability [32]. In all cases, cell survival values were normalised against untreated controls.

Briefly, 96 well-plates were seeded using 5000 cells per well; the plates were left in the incubator at 310 K for 48 h in drug-free medium. After this time, the lectins were added at multiple concentrations. The stock solutions and the corresponding dilutions were prepared using medium supplemented with only 1% of foetal calf serum to ensure that no lectin deactivation occurred by non-selective protein binding [33]. The drug exposure time was 24 h. After this, the drug-containing medium was removed by suction, cells were washed with PBS, and lectin-free medium was added; cells were finally left to recover for 72 h at 310 K. The sulforhodamine B colorimetric assay was used to determine cell survival against an untreated control based on the measurement of cellular protein content [32]. This assay relies on the ability of the sulforhodamine B to bind electrostatically to basic amino acid residues of proteins from fixed cells. The sulforhodamine B absorbance at 570 nm was recorded on a BioRad iMark 96-well microplate reader. The experiments were carried out as triplicates of duplicates in independent experiments and their standard deviations were calculated.

2.11. Cell cycle studies for A2780 cells

Cell cycle investigations were carried out by flow cytometry using PI staining. Briefly, in a 6 well-plate 1.0×10^6 A2780 cells were seeded and allowed to attach for 24 h at 310 K in a 5% CO_2 humidified atmosphere. Following this, cells were treated with $2 \times IC_{50}$ concentrations of DLasiL for 24 h. After drug exposure, the lectin was removed by suction, cells were washed with PBS, harvested by trypsinization, washed twice with PBS, and centrifuged at 1000 g for 4 min. The cell pellet was then resuspended in cold 70% ethanol and kept in a freezer 253 K for 24 h. Cells were centrifuged, the ethanol removed and cells were washed with PBS, followed by staining with 500 μL of a mixture containing PBS, 100 μL of PI stock solution and 160 μL of RNAse stock solution. The sample was kept in the dark for 30 min, centrifuged and the supernatant removed by suction. Cells were resuspended in fresh PBS and were transferred to a flow cytometry tubes to read the fluorescence emission of PI bound to DNA at 617 nm. The data were analyzed using Flowjo software.

2.12. Induction of apoptosis in A2780 cells

Flow cytometry detection of induced apoptosis in A2780 ovarian cancer cells was carried out using Annexin V-FITC and propidium

iodide (PI) staining (BioVision Annexin V Apoptosis Detection Kit). Briefly, 1.0×10^6 cells were seeded on a 6-well plate in triplicate and allowed to attach for 24 h in drug-free medium at 310 K. Cells were then treated with DLasiL for a further 24 h using $2 \times IC_{50}$ concentrations. These experiments used staurosporine (Sigma Aldrich, UK) as a positive control. After the drug exposure period, the supernatant was removed by suction, the cells washed with PBS, trypsinized, centrifuged at $1000 \times g$ for 4 min, and the cell pellet further washed with PBS twice. In order to stain the cells, the pellets were resuspended in 500 μL of a mixture of PBS containing 10 μL of PI/sample and 5 μL of Annexin/sample. Cells were incubated in the dark at ambient temperature for 30 min and then analyzed using a flow cytometer Becton Dickinson FACScan reading in Annexin V-FITC in the FL-1 green channel and PI in the FL-2 red channel for fluorescence detection.

2.13. Caspase 9 activity assay

Caspase 9 induction in A2780 cell lysates was determined by a fluorimetric assay (BioVision, UK) according to the manufacturer's instructions. The experiment included cells exposed to DLasiL at $2 \times IC_{50}$ concentration, as well as untreated negative controls and cells exposed to staurosporine as positive control. After a 24 h incubation period, cells were collected, trypsinized and lysed. The samples were split into two tubes, one for protein quantification using a Bradford assay and the other to measure the caspase 9 activity. The assay was based on the detection of the cleavage of substrate LEHD-AFC (AFC: 7-amino-4-trifluoromethyl coumarin). LEHD-AFC emits blue light (λ_{max} = 400 nm); upon cleavage of the substrate by caspase-9 or related caspases, free AFC emits a yellow-green fluorescence (λ_{max} = 505 nm). All values, determined as triplicates of triplicates, were normalised to protein content and their standard deviations were calculated.

2.14. Confocal microscopy

A2780 ovarian carcinoma cells were seeded in 4-well microscopy chambers (10,000 cells/well; 500 μl supplemented RPMI 1640 medium), left to attach for 24 h, and then treated for another 24 h with different concentrations of DLasiL (0, 0.5 ×, 1 × and 2 × IC_{50}) that was labelled using Alexa fluor 647 (monoclonal antibody labelling kit from Invitrogen; λ_{ex} = 650 nm/λ_{em} = 665 nm). After treatment, medium was removed, cells washed twice with PBS and fixed with 4% paraformaldehyde solution (20 min at RT). Cell nuclei were stained using DAPI (0.1 mg/ml; 10 min at RT; λ_{ex} = 358 nm/λ_{em} = 461 nm) followed by two washes with PBS. Cells were imaged using a Leica SP5 confocal microscope.

3. Results

We investigated the structural and physicochemical properties of DLasiL using tandem mass spectrometry, EPR, ICP-MS, CD and fluorescence emission spectroscopy, which, to the best of our knowledge, comprises the first detailed physical characterisation of the DLasiL lectin. We have compared these data to other relevant lectins, ConBr, ConM and DSclerL, and have explored their anticancer activity towards several cancer cell lines. Additionally, we have investigated the mechanism of the antiproliferative activity of DLasiL lectin.

3.1. Structural investigations

We determined the amino acid sequence, metal content, tryptophan accessibility/microenvironment and thermal stability of DLasiL lectin. Tandem mass spectrometry analysis of sets of overlapping peptides obtained by proteolytic digestions allowed 89% of the amino acid sequence of DLasiL to be determined (Supporting information Table S1). This was confirmed and completed by cloning and sequencing the lectin gene. The protein sequence (Fig. 1) shows a high degree of identity with other Diocleinae lectins. DLasiL is therefore likely to also form homotetramer, with each of the 4 subunits (α-chain) containing 237 amino acids distributed between two chains: β-chain (residues 1–118) and γ-chain (residues 119–237; Supporting information, Table S1). Furthermore, the isotope-averaged molecular masses calculated for the full-length α-chain (25,410 Da) and its derived β- (12,816 Da) and γ- (12,611 Da) fragments are in excellent agreement with the reported experimentally-determined mass [22].

Most lectins are metal-dependent proteins, often containing Mn(II) and Ca(II) ions. We obtained the six-line EPR spectra typical of Mn(II) in aqueous solutions of ConBr, ConM, DSclerL and DLasiL (0.4 mM), thus confirming the presence of paramagnetic Mn(II) in all four lectins (Supporting Fig. S1). Additional ICP-MS measurements were used to obtain quantitative information on Mn content and that of other EPR silent metals (e.g. Mg, Ca). Mg, Mn and Ca were found in significant amounts in all four lectins (Supporting information Table S2). The highest amount of Mn was found in DSclerL (ca. 3 Mn per subunit), followed by ConBr and ConM (ca. 1 Mn per subunit), and DLasiL (lower than 0.5 per subunit; Fig. 2, Table S2).

Fluorescence emission studies were carried out in order to obtain information about the solvent accessibility of the tryptophan residues in relation to conformational flexibility in the DLasiL lectin. The stability of the DLasiL lectin with respect to denaturation by guanidinium hydrochloride (Gdn-HCl) was investigated. DLasiL lectin exhibited a maximum emission at 334 nm that is assigned mainly to the fluorescent tryptophan residues in the folded protein, upon excitation at 280 nm (Supporting information Fig. S2), while the maximum emission was red-shifted to 352 nm upon denaturation with Gdn-HCl. A more detailed investigation of tryptophan accessibility and the polarity of its microenvironment in both native and denatured DLasiL lectin was carried out by using CsCl, KI and acrylamide as cationic, anionic and neutral quenchers, respectively (Table S3, Figs. S3 and S4). DLasiL experienced a strong fluorescence suppression on interaction with acrylamide (56%), followed by iodide (44%) and cesium (30%) as shown by Stern-Volmer plots (see Supporting information Fig. S3). A similar trend in fluorescence quenching of denatured DLasiL lectin was observed (Supporting information Fig. S4). The near-UV CD spectrum of the native DLasiL lectin was recorded in buffered solution at 298 K (Fig. 3). This spectrum exhibited two positive absorption bands at ca. 285 and 290 nm that arise from contributions of the side chains of tryptophan and tyrosine residues. The thermostability of DLasiL lectin in phosphate buffer was investigated in the near-UV region by monitoring the CD signal at 290 nm in the temperature interval 303 to 363 K (Fig. 3A). A denaturation midpoint was observed at 345 K, in agreement with a previous study in which the far-UV region was monitored [22]. The CD spectra acquired in the near-UV region at different temperatures showed a similar pattern of stability compared to that observed in the far-UV region and the variable-temperature experiments at 290 nm (Supporting Fig. S5).

Fig. 3B shows the CD spectrum of native DLasiL in the near-UV region overlaid with that in the presence of 100 mM glucose or 100 mM mannose. There were no significant changes in the near-UV CD spectra of DLasiL upon addition of these sugars, suggesting that sugar binding does not have a major effect on the conformation of the lectin.

Some of the above observations may be rationalized by inspecting the 3D structures of DLasiL and the other lectins that are included for comparison. The structure of DLasiL (Figs. 4 and S6) was modelled on that of *Dioclea guianensis* lectin (pdb 1H9W), which has 96% sequence identity to DLasiL. The Ca/Mn site contains four ligands for Ca (E8, H24, D10 and D19), while the latter two aspartates form bridges and bind also to Mn. The latter is in addition bound to residue N14 and the backbone carbonyl oxygen of Y12. This dinuclear site is adjacent to the surface sugar-binding site (Fig. 4(A)).

Importantly, analysis of dimeric and tetrameric assemblies (Fig. S6, based on the X-ray structure of ConBr; pdb 4H55) suggested that W88 is less exposed to solvent when the lectin oligomerises, with implications

```
                  8     14   19   24                40
DLasiL            ADTIVAVELDSYPNTDIGDPSYPHIGIDIKSIRSKATARWNMQTGKVGTAHISYNSVAKR
DGuiaL            ADTIVAVELDSYPNTDIGDPSYPHIGIDIKSIRSKSTARWNMQTGKVGTAHISYNSVAKR
DSclerL           ADTIVAVELDSYPNTDIGDPNYPHIGIDIKSIRSKSTARWNMQTGKVGTVHISYNSVAKR
DGranL            ADTIVAVELNSYPNTDIGDPNYPHIGIDIKSIRSKSTARWNMQTGKVGTVHISYNSVAKR
ConBr             ADTIVAVELDTYPNTDIGDPSYPHIGIDIKSVRSKKTAKWNMQNGKVGTAHIIYNSVGKR
ConM              ADTIVAVELDTYPNTDIGDPSYPHIGIDIKSVRSKKTAKWNMQNGKVGTAHIIYNSVGKR
                  *********::*********.**********:*** **:****.*****.** ****.**

                                          88          99         109    117
DLasiL            LSAVVSYSGTSSTTVSYDVDLNNVLPEWVRVGLSATTGLYKETNTILSWSFTSKLKTNSI
DGuiaL            LSAVVSYTGSSSTTVSYDVDLNNVLPEWVRVGLSATTGLYKETNTILSWSFTSKLKTNSI
DSclerL           LSAVVSYSGSSSTTVSYDVDLNNVLPEWVRVGLSATTGLYKETNTILSWSFTSKLKTNSI
DGranL            LSAVVSYSGSSSTTVSYDVDLNNVLPEWVRVGLSATTGLYKETNTILSWSFTSKLKTNSI
ConBr             LSAVVSYPNGDSATVSYDVDLDNVLPEWVRVGLSASTGLYKETNTILSWSFTSKLKSNST
ConM              LSAVVSYPNGDSATVSYDVDLDNVLPEWVRVGLSASTGLYKETNTILSWSFTSKLKSNST
                  *******.. .*:*********:**************:**********:**

                   122     131     138
DLasiL            ADANSLHFSFNQFSQNPKDLILQGDATTDSDGNLQLTRVSSDGSPQGSSVGRALFYAPVH
DGuiaL            ADANSLHFSFNQFSQNPKDLILQSDATTDSDGNLELTKVSSSGDPQGSSVGRALFYAPVH
DSclerL           ADENSLHFSFHKFSQNPKDLILQGDAFTDSDGNLQLTKVSSSGDPQGNSVGRALFYAPVH
DGranL            ADANSLHFSFHQFSQNPKDLILQGDAFTDSDGNLELTKVSSSGDPQGNSVGRALFYAPVH
ConBr             HETNALHFMFNQFSKDQKDLILQGDATTGTEGNLRLTRVSSNGSPQGSSVGRALFYAPVH
ConM              HETNALHFVFNQFSKDQKDLILQGDATTGTDGNLELTRVSSNGSPQGSSVGRALFYAPVH
                   : *:*** *::**:: ******.** *.::***.**:***.*.***.************

                   182                       208                 228
DLasiL            IWEKSAVVASFDATFTFLIKSPDRDPADGITFFIANTDTSIPSGSGGRLLGLFPDAN
DGuiaL            IWEKSAVVAGFDATFTFLIKSPDRDPADGITFFIANTDTSIPSGSGGRLLGLFPDAN
DSclerL           IWEKSAVVASFDATFTFLIKSPDREPADGITFFIANTDTSIPSGSGGRLLGLFPDAN
DGranL            IWEKSAVVASFDATFTFLIKSPDREPADGITFFIANTDTSIPSGSGGRLLGLFPDAN
ConBr             IWESSAVVASFEATFTFLIKSPDSHPADGIAFFISNIDSSIPSGSTGRLLGLFPDAN
ConM              IWESSAVVASFDATFTFLIKSSDSHPADGIAFFISNIDSSIPSGSTGRLLGLFPDAN
                  ***.*****.*:*********.* .*****:***:* *:****** ***********
```

Fig. 1. CLUSTAL 2.1 multiple sequence alignment for lectins DLasiL, DGuiaL, DSclerL, DGranL, ConBr, and ConM. Residues involved in the canonical binuclear Ca/Mn site are highlighted in grey: E8, H24, D10 and D19 bind Mn, D10 and D19 also bridge to Ca, which is also bound by N14 and by the backbone oxygen of Y12. Residues involved in carbohydrate binding are shown in orange, and tryptophan residues are highlighted in green. Highlighted in yellow are loop residues 117–122, and residue 131. The loop is disordered in some lectin structures (e.g. DGuiaL, pdb 1H9W, template for homology modelling), and it is thought that the nature of residue 131 plays a role in ordering this loop. An ordered loop indicates a more stabilised interface. The location of the loop is quite close to Trp88 (W88); its flexibility may also directly affect W88 solvent exposure. Residues K138 and D139 (cyan) from the second monomer come into the vicinity of W88 upon dimerisation. (For interpretation of the references to color in this figure legend, the reader is referred to the web version of this article.)

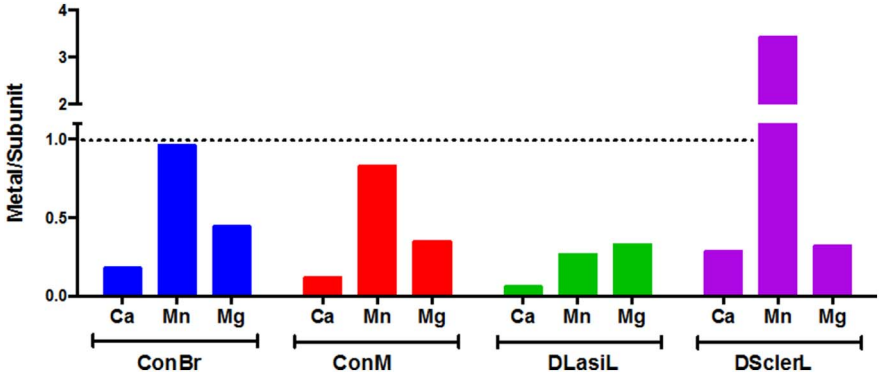

Fig. 2. Stoichiometric ratio for the most abundant metals per lectin protein subunit as determined by ICP-MS.

for protein tryptophan fluorescence discussed later. Moreover, other weak Mn binding sites at the interface between monomers are observed in the X-ray structure of *D. guianensis* lectin (pdb 1H9W) and might explain the binding of > 1 Mn per subunit in DSclerL (weak sites). The low Mn content in our DLasiL samples might weaken the oligomerisation and increase the monomer population, which is expected to affect Trp88 fluorescence.

3.2. Biological studies

3.2.1. Cell viability assays

We determined the antiproliferative activity of lectins ConBr, ConM, DLasiL and DSclerL towards a variety of human cancer cell lines of breast, ovarian, lung and prostate origin, Table 1. In general, all lectins showed potent anticancer activity towards the A2780, A549, and PC3 cell lines, with all IC_{50} values in the nanomolar range varying from 52 to 529 nM. There are no clear trends in the comparative potency of the four lectins in the three cell lines tested. Nonetheless, it appears that the highest activity is achieved in A2780 human ovarian cancer cells. IC_{50} values determined as ranges with 95% confidence intervals are in the Supplementary Information, Table S4. Particularly, DLasiL exhibited the lowest IC_{50} value of 52 ± 2 nM. We also tested DLasiL towards the MCF7 breast cancer cell line and determined its IC_{50} value to be 275 nM.

3.2.2. Cell cycle analysis

In the antiproliferative activity experiments carried out (vide supra), DLasiL exhibited the highest potency towards A2780 ovarian cancer cells, hence we investigated the cellular behaviour of the lectin in this cell line. In particular, we used flow cytometry to investigate the effect of the lectin on the cell cycle of the ovarian cancer cells (Fig. 5).

Flow cytometry analysis of negative untreated controls of A2780 ovarian cancer cells were carried out. As expected, most of the cell population of the corresponding FL-2 histogram is located in the G1 phase (71 ± 1%) while percentage of cells in the S and G2/M phases are 19.1 ± 0.5% and 9 ± 1%, respectively. As a positive control, we determined the percentages of cell population in samples treated with the clinical anticancer drug cisplatin (CDDP). In this case, we observed

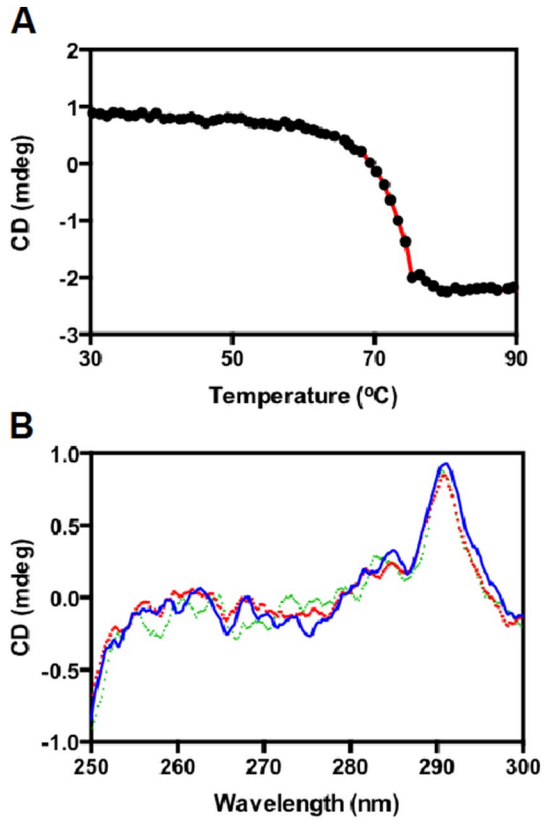

Fig. 3. Circular dichroism spectroscopy of DLasiL in 10 mM phosphate buffered saline at 298 K in the near-UV region. A) Thermal unfolding of DLasiL monitored at 290 nm from 303 to 363 K. B) Effect of the addition of binding sugars at 298 K: native DLasiL (blue solid line), DLasiL + 100 mM glucose (red dashed line) and DLasiL + 100 mM mannose (green dashed line). (For interpretation of the references to color in this figure legend, the reader is referred to the web version of this article.)

a sharp increase in the S phase population up to 50 ± 3% while the G1 phase is reduced to 16.1 ± 0.8%. Population in the G2/M phase accounted for 33 ± 9%. The observed S phase arrest caused by cisplatin is a well-established effect of this platinum drug. It is a result of a mechanism of action that involves covalent binding and the subsequent structural modification of the DNA double helix.

In comparison, A2780 cells treated with 2 × IC_{50} equipotent concentrations of DLasiL for 24 h showed a significant reduction of the G1 phase population to 57.1 ± 0.3%. This is a result of an increase in the G2/M phase (to 22.0 ± 0.6%) with p = 0.001. Meanwhile, changes in the S phase (up to 20.8 ± 0.6%) are minor, but still statistically relevant (p = 0.024).

3.2.3. Induction of apoptosis in A2780 cells

According to the cell cycle analysis, in which lectin DLasiL induces a G2/M arrest in the ovarian cancer cells upon 24 h exposure to 2 × IC_{50} concentrations, and given that lectins with similar behaviours exert their antiproliferative activity by inducing apoptosis, we decided to investigate the induction of this programmed cell death in A2780 cells.

The labelling of cells with Annexin V-FITC/PI (propidium iodide) generates the fluorescence patterns detected by flow cytometry for four distinct cell populations shown in Fig. 6. A bidimensional dot plot can then be divided into four quadrants coded as Q1, Q2, Q3 and Q4. Q1 is associated with non-viable cells, which have lost membrane integrity and are located in the upper left quadrant. They show low fluorescence for annexin V-FITC but a high reading in the FL-2 red channel corresponding to PI. Q2 is associated to late apoptotic cells located in the upper right quadrant, positively labelled by annexin V-FITC and PI. These cells have lost the symmetry of the phosphatidylserine membrane and have further lost membrane integrity. Q3 represents early apoptotic cells found in the lower right quadrant, which show high annexin V FITC fluorescence in the FL-1 green channel but no detectable PI signal in the FL-2 red channel. Q4 is constituted by a group of viable cells that

Table 1
Antiproliferative activity of lectins ConBr, ConM, DLasiL and DSclerL against human A2780 ovarian, A549 lung, MCF-7 breast and PC3 prostate cancer cells. The experiments included 24 h of drug exposure and 72 h of recovery time in drug-free medium. All values were determined as duplicates of triplicates in independent experiments and their standard deviations were determined.

Lectin	IC_{50} (nM)			
	A2780	A549	MCF-7	PC3
ConBr	108 ± 14	95 ± 14	1146 ± 24	529 ± 8
ConM	67 ± 2	62 ± 4	1382 ± 17	176 ± 2
DLasiL	52 ± 2	224 ± 10	275 ± 4	167 ± 1
DSclerL	64 ± 4	102 ± 8	1250 ± 9	264 ± 1

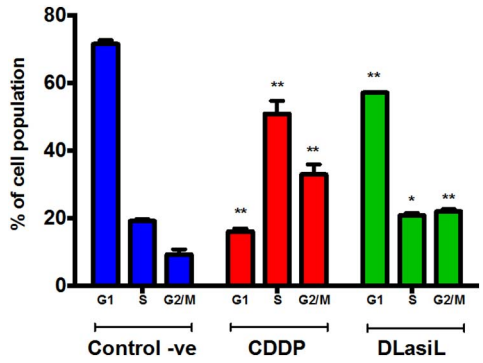

Fig. 5. Flow cytometry analysis of A2780 ovarian cancer cells exposed to 2 × IC_{50} concentrations of DLasiL or cisplatin. The bar chart represents the percentage of cell population in each of the cell cycle phases, G1, S and G2/M determined after propidium iodide staining. The experiments included 24 h of drug exposure and no recovery time in drug-free medium. Statistical significance was evaluated using a Welsh test against untreated negative controls (* $p < 0.05$, ** $p < 0.01$). Values are expressed as means and standard deviation of two independent experiments performed in duplicate.

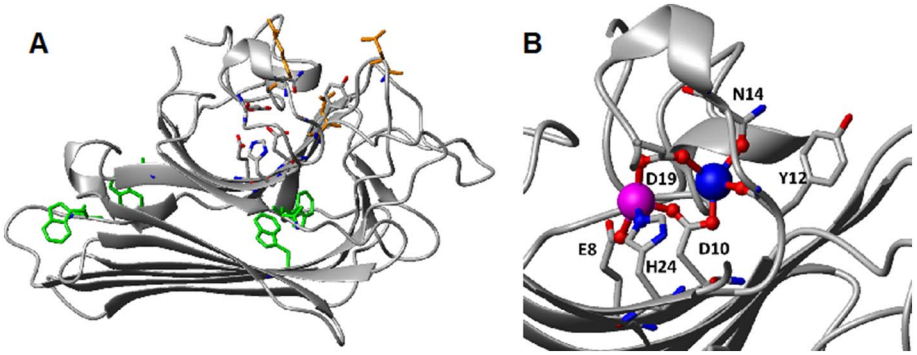

Fig. 4. A) Monomeric homology model of DLasiL, based on the X-ray structure of *D. guianensis* seed lectin (DGuiaL; pdb 1H9W, 96% identity). The backbone is shown in grey, tryptophan residues in green, sugar-binding residues in orange, and atom-colored (CPK) sticks for residues involved in metal binding. B) Closeup of canonical binuclear Mn/Ca site in leguminous seed lectins as predicted for DLasiL, using DGuiaL (pdb 1H9W) as example. Mn is shown in magenta, and Ca in blue. Coordinating water molecules are not shown. (For interpretation of the references to color in this figure legend, the reader is referred to the web version of this article.)

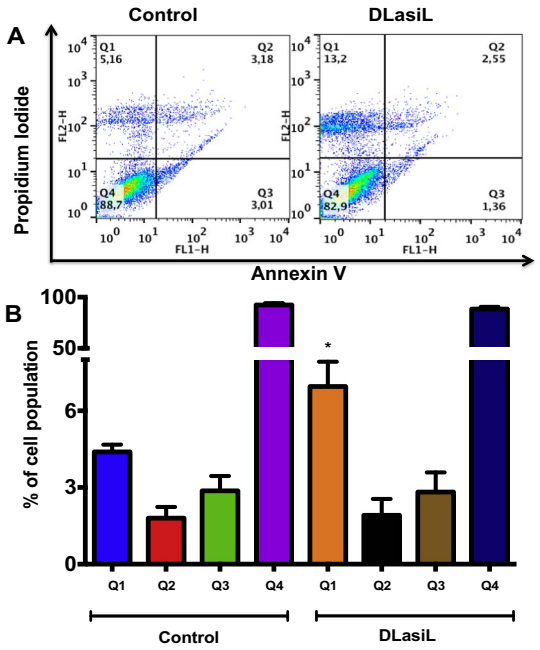

Fig. 6. Flow cytometry analysis of A2780 ovarian cancer cells exposed to DLasiL using fluorescence labelling with annexin V-FITC and propidium iodide. A) Dot plot of negative controls and 24 h lectin-exposed cells B) Bar chart of the percentages of cell population in each of the quadrants of the flow cytometry dot plots (Q1: non-viable, Q2: late apoptotic, Q3: early apoptotic and Q4: viable cells). Statistical significance against the negative untreated control was evaluated using Welch's test with * $p < 0.05$, ** $p < 0.01$, *** $p < 0.001$. Values were determined as the means for triplicate experiments and their standard deviations were calculated.

are located in the lower left quadrant and have not been labelled by annexin nor propidium iodide. As expected, untreated cells were mostly viable (92 ± 2%), with small populations of early and late apoptotic and non-viable cells (4.3 ± 0.2, 1.8 ± 0.4 and 2.8 ± 0.6, respectively). Treatment of A2780 cells with DLasiL led to a small increase in the population of non-viable cells, but the populations of early and late apoptotic remained unchanged.

3.2.4. Caspase 9 activity

To confirm that the mechanism of action of lectin DLasiL involves the activation of apoptosis, we investigated whether increased levels of the apoptotic initiator caspase 9 were observed after exposure to the lectin, Fig. 7. A2780 ovarian cancer cells were treated with DLasiL (2 × IC_{50} concentration) or with staurosporine (as a positive control, well-known to induce apoptosis), and the levels of caspase 9 were measured by the fluorescence detection of the cleavage of substrate LEHD-AFC (AFC: 7-amino-4-trifluoromethyl coumarin). A 45% increase in the level of caspase 9 produced by 24 h exposure to lectin DLasiL compared to the negative controls was observed (Fig. 7).

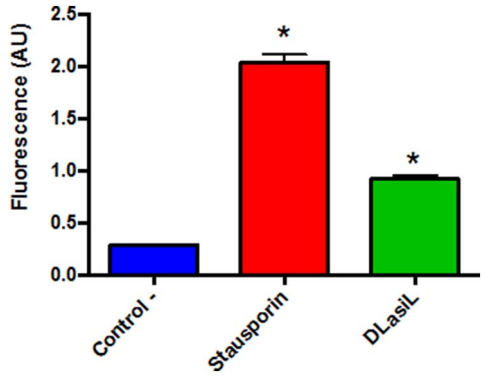

Fig. 7. Caspase 9 activation in A2780 ovarian cancer cells. Cells were treated with DLasiL (2 × IC_{50} concentration), staurosporine as a positive control, or were untreated as negative controls. Statistical significance was evaluated using a Welsh test against the untreated controls (* $p < 0.05$). Values are expressed as means and standard deviation of triplicates.

3.2.5. Confocal microscopy

The cellular distribution of DLasiL lectin was explored using confocal microscopy. Imaging of A2780 carcinoma cells treated with different concentrations (0–2 × IC_{50}) of fluorescent Alexa fluor 647-labelled DLasiL showed that the protein accumulated in cells in a concentration-dependent manner (Fig. 8, stacks A–D). The protein is distributed around the periphery of the nuclei (stained using DAPI). No colocalisation between the fluorescent protein and DAPI was observed (even at the highest concentration used, 2 × IC_{50}; Fig. 8; stacks A–D; Figs. S7–S10; Videos S1–S4). Additionally, high concentrations of the lectin led to morphological changes in treated cells. A2780 cells treated with 2 × IC_{50} of DLasiL were more widely spread and had enlarged nuclei when compared with untreated cells or cells treated with low concentrations of the protein.

4. Discussion

Although lectins purified from various Diocleinae subtribe seeds show only minor differences in their amino acid sequences, their biological activities can differ significantly [14]. These differences in activities are mostly due to the relative positions of the carbohydrate binding sites, and the dimer to tetramer balance, which is pH-dependent. For example, substitution of only two amino acid (D58 and A70) associated with the carbohydrate binding site is responsible for a more opened binding site in the *Canavalia brasiliensis* lectin (ConBr) compared with the *Canavalia ensiformis* lectin (ConA) [14,34]. We determined the amino acid sequence of DLasiL and compared it through sequence alignment with other Diocleinae lectins previously characterized (Fig. 1). This showed a high degree of sequence similarity between the four lectins isolated and analyzed in this work (ConBr, ConM, DSclerL and DLasiL), with the DLasiL and DSclerL amino acid sequences differing only in 12 residues (Fig. 1). However, the moderate change in amino acid composition still promoted significant differences in chemical properties (e.g. metal contents and fluorescence) and biological activity.

Plant lectins require divalent metals (Ca(II) and Mn(II) ions or others e.g. Mg(II)) for their function. Their role seems to be essentially structural, especially for creating the sugar-binding sites [35–37]. DLasiL lectin contained the lowest levels of these metal ions (Fig. 2 and Table S2; see details in Supporting information), which, given the complete conservation of metal-binding residues (Figs. 1 and 3(B)) and the uniform protocol for protein purification, could be due to differences in plant growth or soil conditions, or to subtle differences in inherent chemical properties due to the small differences in primary sequence. The Mn contents of DSclerL were surprisingly high, but it is noted that the X-ray structure of DGuiaL (pdb 1H9W) shows several weak Mn sites at the interface between monomers. Most notably, H180 (a neighbor of W88; see below) is bound to a Mn ion, with two ordered water molecules, one of which forms an H-bond to a backbone nitrogen in the adjacent monomer (Fig. S6). Thus, in terms of both structural stability of individual monomers, and of stability of the tetramer, it is conceivable that metal contents and structural stability are correlated – in turn, the lower the metal content, the more flexible and dynamic the protein will behave. It is likely that such differences in dynamic properties play important roles in the biological activity of lectins. It may be noted that the medium used for all biological assays with DLasiL was supplemented with Mn(II), Ca(II) and Mg(II) in an attempt to ensure that all metal binding sites on the protein were saturated.

Fluorescence studies showed that DLasiL lectin exhibited a maximum emission at 334 nm when excited at 280 nm, which suggests a more polar environment for tryptophan residues compared to other

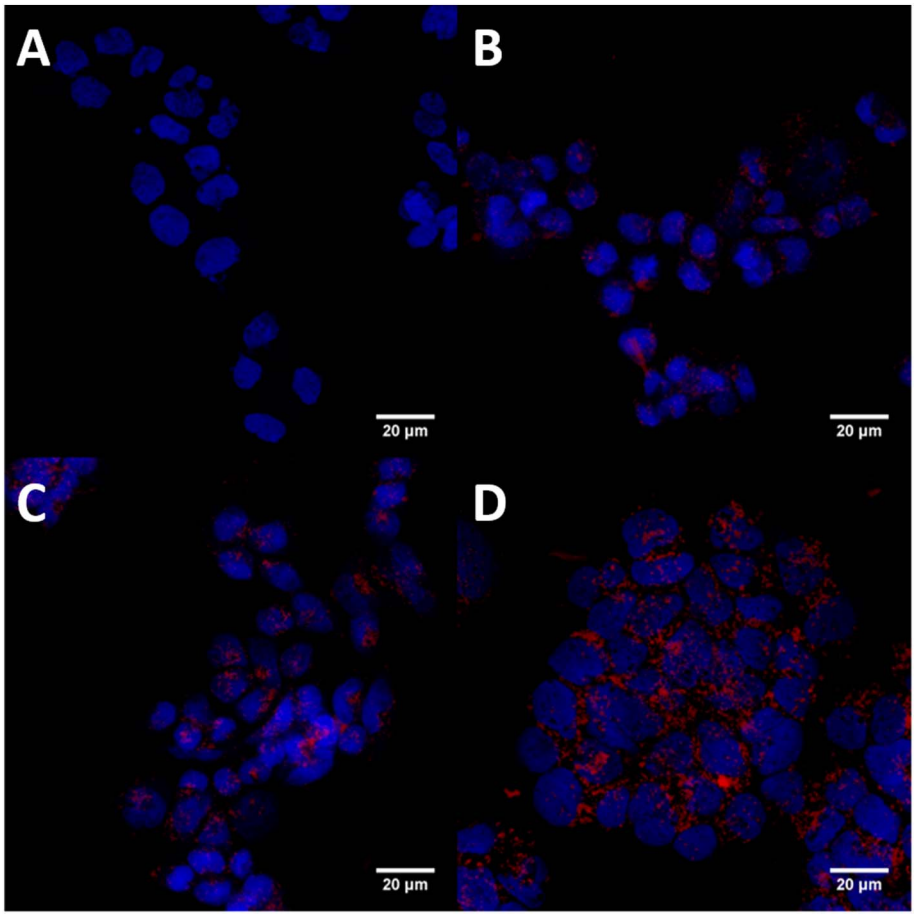

Fig. 8. Z projection of confocal images of A2780 ovarian carcinoma cells treated for 24 h with: A) negative control; B) 0.5 × IC_{50} DLasiL; C) 1 × IC_{50} DLasiL; D) 2 × IC_{50} DLasiL. DLasiL was labelled with Alexa fluor 647 (red); nuclei stained with DAPI (blue). (For interpretation of the references to color in this figure legend, the reader is referred to the web version of this article.)

lectins [27]. All four DLasiL tryptophan residues are fully conserved in all lectins under study here, as well as in DGuiaL. This is also true for their immediate environments [29,38]. Inspection of these environments reveals that W40 and W109 are fairly buried and surrounded by largely hydrophobic residues (W40: L9, I25, M42, V65, Y67 and F197; W109: V91, L93, F111, F128, F130, F133, V140 and F212), that W182 is fairly solvent-exposed, with only the polar N82, S185 and the small A186 as neighbors, and that the environment of W88 is also quite polar: It forms a stacking interaction with H180 from the same monomer, and in the dimer or tetrameric forms only, K138 and D139 from a second monomer enter its vicinity. Thus, in a multimeric state, W88 is clearly more buried than in the monomer. Furthermore, W40 is close to the dinuclear metal binding site (ca. 10 Å), so its accessibility may be affected by the protein's metalation state. We suggest that the more polar tryptophan environment observed for DLasiL may be an indication for higher structural flexibility and/or a lower degree of tetramerisation – which would also be in keeping with the lower metal contents of our preparation that may lead to decreased conformational stability and oligomerisation.

More detailed measurements carried out using CsCl, KI and acrylamide as fluorescence quenchers showed that acrylamide is the most effective suppressor of the native DLasiL fluorescence, followed by iodide (Table S3, Fig. S3), while Cs(I) quenched less efficiently. These results might indicate that the neutral acrylamide and anionic I^- quenchers have more access to the tryptophan residues than the cationic quencher Cs(I). It may be suggested that the three different fluorescence quenchers target different tryptophans to different degrees. Access by Cs(I) may be largely confined to W182, as the microenvironments of W40 and W109 are probably too hydrophobic, and access to W88 may be, at least in the dimer/tetramer, partially restricted due to the presence of both K138 and potentially a weakly bound Mn ion. The residue W88 could be further explored as an interesting probe for monomer-dimer equilibrium studies.

The maximum emission wavelength shifted to 352 nm upon denaturation with guanidinium hydrochloride (Gdn-HCl), which is typical of tryptophan residues fully exposed to water as consequence of protein unfolding. As expected, the extent of fluorescence quenching was higher for denatured DLasiL (Table S3, Fig. S4), since the accessibility of the quenchers to the tryptophan residues is increased in the unfolded lectin. The results obtained with the denatured lectin were also consistent with a neutral and positively accessible tryptophan microenvironment, as shown by the Stern-Volmer analysis (Table S3 and Figs. S3 and S4).

The circular dichroism (CD) spectra of proteins depend on their secondary structure and conformation. Therefore, this technique provides structural information on proteins, and can be used to study conformational changes due to binding of ligands, temperature, denaturants, mutations, etc. We have reported previously the relative β-sheet and α-helical content of native DLasiL (40.2% antiparallel β-sheet, 4.6% parallel β-sheet, 7.2% α-helices, 17.3% turns, and 28.7% unordered structure), and studied its thermal stability in the far-UV range by using CD spectroscopy [22]. The high thermal stability observed for DLasiL is a common feature of legume lectins in general [39], and makes them attractive proteins for biotechnological purposes.

So far, a few lectins have shown anticancer activity in vitro and in vivo, and are reported to bind to cell membranes of cancer cells or to their receptors, causing cytotoxicity, apoptosis and inhibition of tumour growth [7]. The binding affinity of lectins for various glycans and glycoproteins on the cell wall is well described elsewhere [40]. Ligand binding can affect the tertiary structure of a protein. Therefore, we employed CD spectroscopy to study the binding of different carbohydrates to DLasiL lectin. Two positive absorption bands with maximum

wavelengths at ca. 290 nm and 285 nm were observed. These bands arise from contributions of the side chains of tyrosine and tryptophan residues. We observed only minor changes in the near-UV CD spectrum of DLasiL on incubation with glucose or mannose under the experimental conditions employed (Fig. 3B). This result showed that the binding of these carbohydrates has little effect on the tertiary structure of native DLasiL. This is expected since the divalent metals binding organize the sugar binding site, which is not further altered.

Interestingly, DLasiL showed the highest antiproliferative activity towards A2780 cells of the lectins tested (IC_{50} 52 ± 2 nM), followed by DSclerL (IC_{50} 64 ± 4 nM), ConM (IC_{50} 67 ± 2 nM) and ConBr (IC_{50} 108 ± 14 nM) (Table 1). DLasiL and DSclerL exhibited higher activity in the A2780 ovarian cell line than in A549 lung, or PC3 prostate cells, with IC_{50} values in the range of 100–275 nM in the latter. The other lectins tested showed a similar behaviour, and the potency of ConBr is 5-fold lower in the PC3 cells when compared to A2780 and A549 cells (IC_{50} values 529 ± 8, 108 ± 14 and 95 ± 14 nM, respectively). Lectin binding affinity to various glycans and glycoproteins varies in different tumours, because of the distinct carbohydrates moieties on their surface [33,40]. Therefore, these changes observed in the antiproliferative activity might suggest the differential recognition of glycan-structures contained within the different cell lines studied. According to Packer et al., ovarian cancer cells show moieties with high mannose content as the most abundant structures amongst other *N*-glycans subgroups [41]. Plant lectins including those studied here, are thought to be glucose/mannose selective binders, which supports this hypothesis.

More detailed cellular studies were conducted with DLasiL involving cell cycle and apoptosis studies. The mammalian cell cycle is well studied by measuring changes in the cellular DNA content through transitions in different cellular growth phases, such as G1, S and G2/M. Cellular DNA content can easily be measured by detecting propidium iodide (PI) fluorescence, as this organic dye intercalates quantitatively into DNA. The FL-2 flow cytometry histograms show 3 sections, 2 major peaks corresponding to G1 and G2/M stages with one and two copies of DNA correspondingly, and a third section bridging the two previous ones which represents cells in S phase with the cell population undergoing duplication of DNA [42,43]. Contrary to cisplatin, in the case of the lectin DLasiL, there is a clear arrest in G2/M phase. This effect on the cell cycle of cancer cells has been previously reported, for instance a series of lectins extracted from mushrooms can induce G2/M arrest of human leukaemia U937 cells in consequence initiate an apoptotic cascade. In this case, the cell cycle arrest may be related to the upregulation of p21/Waf1 and a subsequent decrease in Bcl-2 before cytochrome *c* release into the cytosol and caspase-9 activation [44,45]. In a similar way, an *N*-acetyl-D-glucosamine lectin from *Psathyrella asperospora* is known to cause G2/M cell cycle arrest in HT29 cells by binding to GlcNAc-terminated glycans after 24 h of drug exposure.

Lectins can induce death in cancer cells via different apoptotic pathways [46]. Caspase-9 initiates the intrinsic apoptosis pathway, associated with changes in morphological and biochemical characteristics [47], activating a process that involves other types of caspases such as procaspase-3 and caspase-3 [48].

Apoptosis is often suggested as the mechanism by which plant lectins can induce cell death [46]. Based on several reports, ConA exerts its antiproliferative activity through apoptotic mechanisms which involve binding to glycoproteins of cell membranes. Once it is internalized, it locates preferentially in the mitochondria where it activates a number of signalling pathways [14]. This lectin exhibits high anti-proliferative activity in A375 melanoma cells. In this particular case, its mechanism of action relies on the activation of an apoptotic cascade involving caspase-9 and caspase-3, causing mitochondrial collapse and leading to release of cytochrome *c* into the cytosol [47]. ConA also adheres to Merkel cell skin carcinoma [48], and may also induce mitochondrial apoptosis, BNIP3-mediated mitochondrial autophagy, and eventually causes death of tumour cells [6].

Regarding the investigations of apoptosis induction, we analyzed four distinct populations in A2780 cells exposed to lectin DLasiL under similar conditions to those used in the cell cycle experiments (24 h drug exposure at 2 × IC_{50} concentrations, no recovery time) and compared them to those of untreated controls. As expected, negative controls exhibit most of their cell population in the Q4 quadrant in which viable cells have low fluorescence in both FL-1 green and FL-2 red channels (92 ± 2%). Populations in quadrants Q1, Q2 and Q3 are relatively low and in no case above 5% (Q1: 4.3 ± 0.2, Q2: 1.8 ± 0.4 and Q3: 2.8 ± 0.6). Cells exposed to lectin DLasiL also had most of the population (88 ± 2%). in Q4 while Quadrants Q2 and Q3, which exhibit high Annexin V fluorescence in the FL-1 green channel, remained unchanged with percentages of cell populations of 1.9 ± 0.6 and 2.8 ± 0.7% respectively. Surprisingly, the only statistically relevant change observed ($p = 0.035$) is an increase of the population in Q1 with only high fluorescence in the FL-2 red channel caused by PI intercalation into DNA after the membrane of the cells has been compromised. These results and in particular changes in the Q1 quadrant do not indicate that there is induction of apoptosis in the first 24 h of drug exposure. In contrast, when we investigated the activation of caspase 9 - we observed a 45% increase in fluorescence from the cleavage of substrate LEHD-AFC (AFC: 7-amino-4-trifluoromethyl coumarin) (Fig. 7) which suggests an early activation of an apoptotic cell death. Such is the case of caspase-activated cell death by ConA, another lectin which belongs to the same Diocleinae subtribe [47]. Taken together, these contrasting results open up several possibilities, including the following. First that the activation of the apoptotic cascade does occur within the 24 h of drug exposure, and it is not until the 72 h of cell recovery time in drug-free medium that the cell viability is affected. Hence changes in the phospholipid membrane are not detected under the conditions of our apoptosis experiment. Second, that a different mechanism of cell death could be involved in the antiproliferative activity of DLasiL. The latter is possible as it is recognised that not all caspase activations necessarily lead to apoptotic cell death [49,50]. An example is caspase-3 activation in PHA-stimulated T lymphocytes in the absence of apoptosis [50].

Additionally, confocal microscopy data suggested that DLasiL is localised in the membrane or cytosol of treated cells. Plant lectins are known to attach to the cellular membrane of treated cells and then become internalized, being able to localise in different cellular compartments. For example, ConA targets mitochondria in mice hepatoma cells [51], while WGA is found in lysosomes and trans-Golgi network in human prostate cancer cells [52]. Other lectins such as frutalin, XCL or AAL [53–55] are reported to accumulate around the nuclei of cells, as DLasiL does. Interestingly, frutalin possesses some antiproliferative activity in HeLa cells, and is also capable of altering the cellular morphology and induce apoptosis [53]. However, while frutalin is also found in the nucleus of treated cells, DLasiL is not, indicating differences in their cellular behaviour and, probably, mode of action. Further experiments are required to fully understand the cellular distribution and specific targets of DLasiL leading to the potent antiproliferative activity observed.

5. Conclusions

We report studies of the recently isolated seed lectin DLasiL. Sequence comparisons and homology modelling suggested that its structure is similar to that of related lectins, in particular the conservation of the dinuclear Ca/Mn, sugar- and additional metal binding sites at monomer interfaces. DLasiL lectin showed potent nanomolar activity towards human cancer cell lines, as good or better than the activity of other lectins from the Diocleinae subtribe. Particularly high potency was observed against A2780 human ovarian cancer cells (IC_{50} 52 ± 2 nM). This suggests high affinity of DLasiL towards the glycans, glycoproteins and/or receptors present in the cytosol and/or cell surface of A2780 cells.

Investigations into the cellular basis of the antiproliferative activity of lectin DLasiL showed G2/M cell cycle arrest in A2780 ovarian cancer cells after 24 h exposure, as previously reported for related lectins. Further flow cytometry studies did not show a significant increase in the apoptotic populations within this time frame, but caspase 9 activation was detected, suggesting that DLasiL causes a delayed onset of programmed cell death. Additionally, confocal microscopy studies showed that fluorescently-labelled DLasiL lectin is taken up by A2780 cells in a concentration-dependent manner over the range 0.5–2 × IC_{50}, and is localised around the periphery of the nucleus (but not in the nucleus), perhaps in the cytoplasm and at glycosylation sites in the endoplasmic reticulum. DLasiL treatment caused a marked change in cell morphology, enlarging the nuclei and spreading the cells.

This is the first report of the antiproliferative activity of newly isolated lectins DLasiL and DSclerL. These natural products can be readily isolated and purified from natural sources or produced as recombinant proteins with potential for high specificity. Additionally, lectins might be useful auxiliary agents for the reduction of side effects associated with current chemotherapy and radiotherapy. Lectins are resistant to digestion, survive through the gut, bind to gastrointestinal cells entering in the circulation, and maintain their biological activity [56]. For example, lectins from mistletoe provide an alternative therapy for breast cancer showing a relevant clinical effect in tumour progression throughout survival and recurrences [57]. Overall, the current investigation has led to the discovery of highly potent plant lectins, which might prove to be valuable for cancer treatment in the future.

Abbreviations

DLasiL	lectin protein from *Dioclea lasiocarpa*
ConBr	lectin protein from *Canavalia brasiliensis*
ConM	lectin protein from *Canavalia maritima*
DSclerL	lectin protein from *Dioclea sclerocarpa*
A2780	ovarian cancer cells
A549	lung cancer cells
MCF-7	breast cancer cells
PC3	prostate cancer cells
ICP-MS	inductively coupled plasma- mass spectrometry
EPR	electron paramagnetic resonance
CD	circular dichroism

Competing financial interests

The authors declare no competing financial interests.

Acknowledgments

We thank the Coordenação de Aperfeiçoamento de Nível Superior (CAPES) for providing PhD fellowship for A.C.S.G. including one-year “sandwich fellowship” in the Department of Chemistry at Warwick University CAPES (fellowship for E.H.S.S. to spend one-year at the University of Warwick). The Fundación Barrié, Spain (post-doctoral fellowship for M.J.R.), and support from the ERC (grant no. 247450) and EPSRC (grant no. EP/F034210/1) for PJS.

Appendix A. Supplementary data

Supplementary information accompanies this paper and contained further details of EPR and CD measurements, Tables of MS data on tryptic peptides of DLasiL (S1), metal content of lectins (S2), and Figs. S1 (EPR), S2–S4 (fluorescence), S5 (CD), S6 (models showing seed lectin tetramer and dimer structures, and dependence of the solvent accessibility of W88 on oligomerisation state), S7–S10 (Confocal fluorescence images) and Videos S1–S4 (confocal fluorescence video for cell control and treated with 0.5 ×, 1 × and 2 × IC_{50} DLasiL). Supplementary data associated with this article can be found in the online version, at doi: http://dx.doi.org/10.1016/j.jinorgbio.2017.07.011.

References

[1] R. Siegel, J. Ma, Z. Zou, A. Jemal, CA Cancer J. Clin. 64 (2014) 9–29.
[2] A. Jemal, F. Bray, M.M. Center, J. Ferlay, E. Ward, D. Forman, CA Cancer J. Clin. 61 (2011) 69–90.
[3] A. Thorburn, Apoptosis 13 (2008) 1–9.
[4] H. Ghazarian, B. Idoni, S.B. Oppenheimer, Acta Histochem. 113 (2011) 236–247.
[5] U. Kuzmanov, H. Kosanam, E.P. Diamandis, BMC Med. 11 (2013) 31.
[6] H.Y. Lei, C.P. Chang, J. Biomed. Sci. 16 (2009) 10.
[7] E.G. De Mejia, V.I. Prisecaru, Crit. Rev. Food Sci. Nutr. 45 (2005) 425–445.
[8] A.M. Assreuy, S.R. Fontenele, F. Pires Ade, D.C. Fernandes, N.V. Rodrigues, E.H. Bezerra, T.R. Moura, K.S. do Nascimento, B.S. Cavada, Naunyn Schmiedeberg's Arch. Pharmacol. 380 (2009) 509–521.
[9] H. Rudiger, H.J. Gabius, Glycoconj. J. 18 (2001) 589–613.
[10] G.A. Bezerra, R. Viertlmayr, T.R. Moura, P. Delatorre, B.A. Rocha, K.S. do Nascimento, J.G. Figueiredo, I.G. Bezerra, C.S. Teixeira, R.C. Simoes, C.S. Nagano, N.M. de Alencar, K. Gruber, B.S. Cavada, PLoS ONE 9 (2014) e97015.
[11] D.K. Rieger, A.P. Costa, J. Budni, M. Moretti, S.G.R. Barbosa, K.S. Nascimento, E.H. Teixeira, B.S. Cavada, A.L.S. Rodrigues, R.B. Leal, Pharmacol. Biochem. Behav. 122 (2014) 53–60.
[12] F.R. Holanda, A.N. Coelho-de-Sousa, A.M.S. Assreuy, J.H. Leal-Cardoso, A.F. Pires, K.S. do Nascimento, C.S. Teixeira, B.S. Cavada, C.F. Santos, Protein Pept. Lett. 16 (2009) 1088–1092.
[13] M. Augustin, P.R. Bock, J. Hanisch, M. Karasmann, B. Schneider, Arzneim.-Forsch. 55 (2005) 38–49.
[14] W.W. Li, J.Y. Yu, H.L. Xu, J.K. Bao, Biochem. Biophys. Res. Commun. 414 (2011) 282–286.
[15] E.G. de Mejia, V.P. Dia, Cancer Metastasis Rev. 29 (2010) 511–528.
[16] B. Liu, H.J. Bian, J.K. Bao, Cancer Lett. 287 (2010) 1–12.
[17] E.J.M. Van Damme, N. Lannoo, W.J. Peumans, Adv. Bot. Res. 48 (48) (2008) 107–209.
[18] Z. Shi, N. An, S. Zhao, X. Li, J.K. Bao, B.S. Yue, Cell Prolif. 46 (2013) 86–96.
[19] Q.L. Jiang, S. Zhang, M. Tian, S.Y. Zhang, T. Xie, D.Y. Chen, Y.J. Chen, J. He, J. Liu, L. Ouyang, X. Jiang, Cell Prolif. 48 (2015) 17–28.
[20] M.C. Silva, C.A. de Paula, J.G. Ferreira, E.J. Paredes-Gamero, A.M. Vaz, M.U. Sampaio, M.T. Correia, M.L. Oliva, Biochim. Biophys. Acta 1840 (2014) 2262–2271.
[21] P. Lin, T.B. Ng, J. Agric, Food Chem. 56 (2008) 10481–10486.
[22] A.S. do Nascimento, A.C. Gondim, J.B. Cajazeiras, J.L. Correia, F. Pires Ade, K.S. do Nascimento, A.L. da Silva, C.S. Nagano, A.M. Assreuy, B.S. Cavada, J. Mol. Recognit. 25 (2012) 657–664.
[23] M.M. Bradford, Anal. Biochem. 72 (1976) 248–254.
[24] U.K. Laemmli, Nature 227 (1970) 680–685.
[25] P. Gouet, X. Robert, E. Courcelle, Nucleic Acids Res. 31 (2003) 3320–3323.
[26] A. Pusztai, S. Bardocz, S.W. Ewen, Front. Biosci. 13 (2008) 1130–1140.
[27] N.A.M. Sultan, R.N. Rao, S.K. Nadimpalli, M.J. Swamy, Biochim. Biophys. Acta Gen. Subj. 1760 (2006) 1001–1008.
[28] L.A. Kelley, M.J. Sternberg, Nat. Protoc. 4 (2009) 363–371.
[29] D.A. Wah, A. Romero, F. Gallego del Sol, B.S. Cavada, M.V. Ramos, T.B. Grangeiro, A.H. Sampaio, J.J. Calvete, J. Mol. Biol. 310 (2001) 885–894.
[30] E.H. Bezerra, B.A. Rocha, C.S. Nagano, A. Bezerra Gde, T.R. Moura, M.J. Bezerra, R.G. Benevides, A.H. Sampaio, A.M. Assreuy, P. Delatorre, B.S. Cavada, Biochem. Biophys. Res. Commun. 408 (2011) 566–570.
[31] R. Koradi, M. Billeter, K. Wuthrich, J. Mol. Graph. 14 (1996) 51–55 (29–32).
[32] V. Vichai, K. Kirtikara, Nat. Protoc. 1 (2006) 1112–1116.
[33] E.L. Heinrich, L.A. Welty, L.R. Banner, S.B. Oppenheimer, Acta Histochem. 107 (2005) 335–344.
[34] J. Sanz-Aparicio, J. Hermoso, T.B. Grangeiro, J.J. Calvete, B.S. Cavada, FEBS Lett. 405 (1997) 114–118.
[35] P.C. Harrington, R. Moreno, R.G. Wilkins, Isr. J. Chem. 21 (1981) 48–51.
[36] J. Abhilash, M. Haridas, Appl. Biochem. Biotechnol. 176 (2015) 277–286.
[37] N. Sharon, H. Lis, FASEB J. 4 (1990) 3198–3208.
[38] I.L. Barroso-Neto, P. Delatorre, C.S. Teixeira, J.L. Correia, J.B. Cajazeiras, R.I. Pereira, K.S. Nascimento, E.P. Laranjeira, A.F. Pires, A.M. Assreuy, B.A. Rocha, B.S. Cavada, Int. J. Biol. Macromol. 82 (2016) 464–470.
[39] V.R. Srinivas, G.B. Reddy, N. Ahmad, C.P. Swaminathan, N. Mitra, A. Surolia, Biochim. Biophys. Acta Gen. Subj. 1527 (2001) 102–111.
[40] J.P. Chambers, B.P. Arulanandam, L.L. Matta, A. Weis, J.J. Valdes, Curr. Issues Mol. Biol. 10 (2008) 1–12.
[41] M. Anugraham, F. Jacob, S. Nixdorf, A.V. Everest-Dass, V. Heinzelmann-Schwarz, N.H. Packer, Mol. Cell. Proteomics 13 (2014) 2213–2232.
[42] J.O. Patterson, M. Swaffer, A. Filby, Methods 82 (2015) 74–84.
[43] H.B. Lodish, A. Zipursky, S. Lawrence, Molecular Cell Biology, 4th edition, (2000) (New York).
[44] S.P. Kim, M.Y. Kang, Y.H. Choi, J.H. Kim, S.H. Nam, M. Friedman, Food Funct. 2 (2011) 348–356.
[45] Y. Koyama, T. Suzuki, A. Kajiya, M. Isemura, Int. J. Med. Mushrooms 7 (2005) 201–212.
[46] M. Deepa, T. Sureshkumar, P.K. Satheeshkumar, S. Priya, Chem. Biol. Interact. 200 (2012) 38–44.
[47] B. Liu, M.W. Min, J.K. Bao, Autophagy 5 (2009) 432–433.

[48] K. Sames, U. Schumacher, Z. Halata, E.J. Van Damme, W.J. Peumans, B. Asmus, R. Moll, I. Moll, Exp. Dermatol. 10 (2001) 100–109.
[49] M.C. Abraham, S. Shaham, Trends Cell Biol. 14 (2004) 184–193.
[50] A. Zeuner, A. Eramo, C. Peschle, R. De Maria, Cell Death Differ. 6 (1999) 1075–1080.
[51] C.P. Chang, M.C. Yang, H.S. Liu, Y.S. Lin, H.Y. Lei, Hepatology 45 (2007) 286–296.
[52] R.D. Allen, C.C. Schroeder, A.K. Fok, J. Histochem. Cytochem. 37 (1989) 195–202.
[53] C. Oliveira, A. Nicolau, J.A. Teixeira, L. Domingues, J Biomed Biotechnol (2011) 568932.
[54] L.G. Yu, D.G. Fernig, M.R.H. White, D.G. Spiller, P. Appleton, R.C. Evans, I. Grierson, J.A. Smith, H. Davies, O.V. Gerasimenko, O.H. Petersen, J.D. Milton, J.M. Rhodes, J. Biol. Chem. 274 (1999) 4890–4899.
[55] F. Francis, C. Marty-Detraves, R. Poincloux, L. Baricault, D. Fournier, L. Paquereau, Eur. J. Cell Biol. 82 (2003) 515–522.
[56] U. Valentiner, S. Fabian, U. Schumacher, A.J. Leathem, Anticancer Res. 23 (2003) 1197–1206.
[57] R. Grossarth-Maticek, R. Ziegler, Forsch. Komplementarmed. 13 (2006) 285–292.